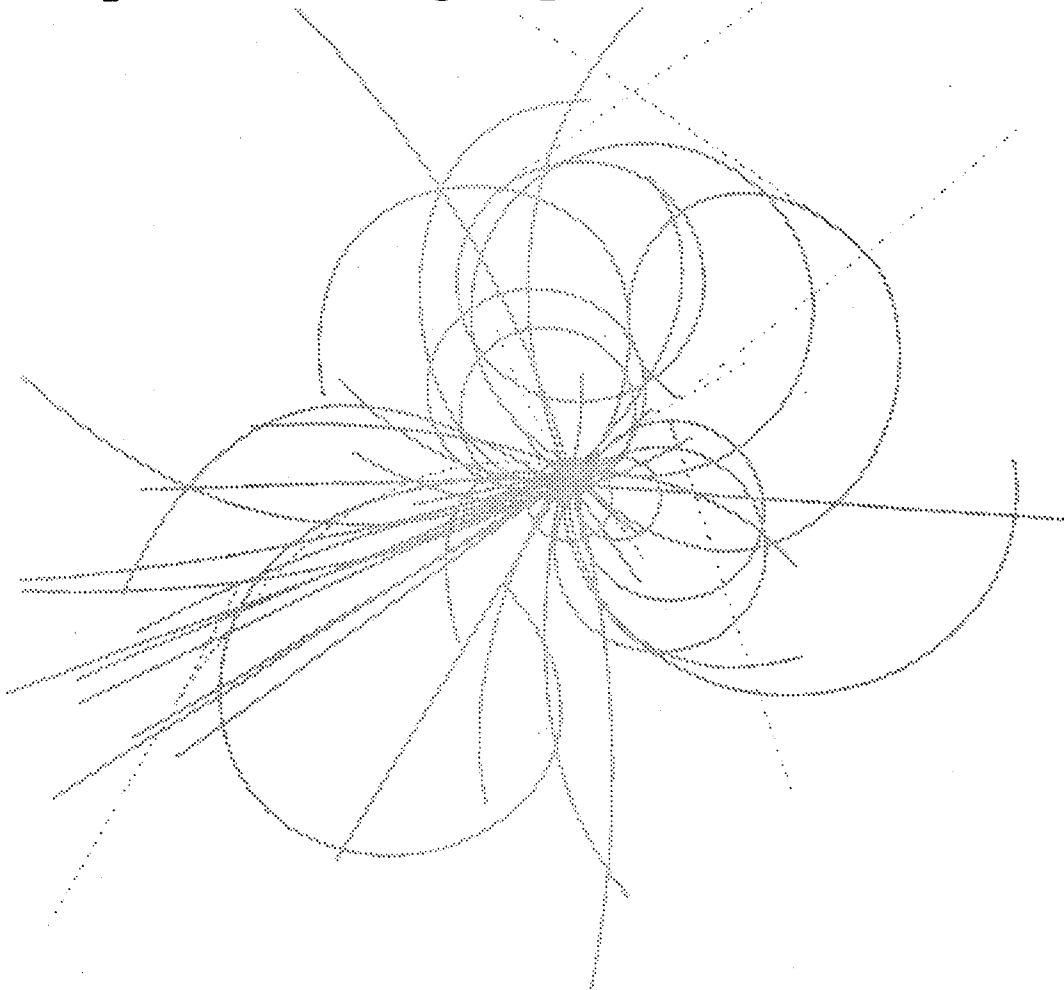


Superconducting Super Collider Laboratory



Cable Keystone Angle Optimization for 40-mm SSC Quadrupole Magnet Development

D.W. Capone, V.A. Bardos, D. Christopherson,
F. Clark, S. Graham, C.R. Hannaford, T.D. Reed, Jr.,
and J. Seuntjens

March 1992

Cable Keystone Angle Optimization for 40-mm SSC Quadrupole Magnet Development*

**D.W. Capone, V.A. Bardos, D. Christopherson, F. Clark,
S. Graham, C.R. Hannaford, T.D. Reed, Jr., and J. Seuntjens**

**Superconducting Super Collider Laboratory[†]
2550 Beckleymeade Avenue
Dallas, Texas 75237**

March 1992

*Presented at the International Industrial Symposium on the Super Collider, New Orleans, March 4–6, 1992.

[†]Operated by the Universities Research Association, Inc., for the U.S. Department of Energy under Contract No. DE-AC35-89ER40486.

CABLE KEYSTONE ANGLE OPTIMIZATION FOR 40-MM SSC QUADRUPOLE MAGNET DEVELOPMENT

D.W. Capone, V.A. Bardos, D. Christopherson, F. Clark, S. Graham,
C. R. Hannaford, T. D. Reed, Jr., and J. Seuntjens

Superconducting Super Collider Laboratory*
2550 Beckleymeade Avenue
Dallas, TX 75237

INTRODUCTION

A series of cables was fabricated meeting all aspects of the latest Superconducting Super Collider (SSC) specification for 30-strand outer cables¹ with the exception of varying the keystone angle between the current specification value of 1.2° and a maximum of 2.2° . In addition, a series of cables with an increased pitchlength is presented. These fabrication experiments have been performed in order to provide an expanded design envelope for the development of quadrupole magnets by the Babcock and Wilcox/Seimens (B&W/S) team. By pushing the cable parameters beyond currently acceptable limits, the B&W/S team will be provided with the data necessary to perform a trade-off between performance, cost, and manufacturability. At the maximum keystone angle of 2.2° , a coil cross section is possible that eliminates the need for wedges in the coil and provides for a simplified magnet manufacturing process. This experiment focuses on the differences identified within each of the cables as the keystone angle is increased. The sections below describe the fabrication details of the cables produced and the metallographic features of the cables. There is also a summary of the electrical and mechanical properties of the as-fabricated cables.

CABLE FABRICATION

All of the cables produced for this study were fabricated from a single batch of strand produced by Oxford Superconducting Technology for use in the dipole magnets for the Accelerator System String Test (ASST) program at the SSC. The properties of 30-strand inner and 36-strand outer cables produced for the ASST program have been described in a companion paper by Christopherson *et al.*² All of the strand for all of the cables was loaded onto the 48-strand cabling machine at Lawrence Berkeley Laboratory^{3,4,5} at the outset of the runs. A new set of turkshead rollers was installed to bring the initial keystone angle of the cables in line with the midpoint of the SSC specification. (Previous runs, as shown in Ref. 2, have been produced near the minimum keystone allowed by the specification in order to minimize the degradation observed in the ASST cables.) In addition, care was taken to seat the rolls properly within the set of roller bearings.

*Operated by the Universities Research Association, Inc., for the U.S. Department of Energy under Contract No. DE-AC35-89ER40486.

The cables were manufactured sequentially, with an effort made to maintain the cable parameters at the midpoint of the specification tolerances for both the cable midthickness and the cable width. The initial runs were 180-m lengths of standard 30-strand outer cable that were supplied to Siemens for a series of winding experiments to initiate its magnet development program. These cables are identified by the standard SSC cable ID convention, SSC-2-O-00052 and SSC-2-O-00053. Following these initial runs, a series of five cables was manufactured using the same cable pitch-length as the standard cable. These five cables were made with the following nominal keystone angles: 1.2°, 1.4°, 1.6°, 1.9°, and 2.2°. These cables are identified as TST-A12, TST-A14, TST-A16, TST-A19, and TST-A22. In addition to the five cables produced with the standard pitch length of 73 mm, three cables were produced with a pitch length of 81 mm. The final three cables had nominal keystone angles of 1.6°, 1.9°, and 2.2°; they are identified as TST-P16, TST-P19, and TST-P22. See Table 1 for properties of the various cable samples.

Table 1. A summary of the cable parameters and variations measured during these experiments.

Cable ID	Keystone Angle (°)	Std. Dev. (°)	Mid-thick. (in.)	Std. Dev. (in.)	Width (in.)	Minor Edge (in.)
SSC-2-O-00052	1.193	0.005	0.04591	0.00002	0.38370	0.04192
SSC-2-O-00053	1.188	0.005	0.04591	0.00003	0.38375	0.04193
TST-A12	1.199	0.013	0.04590	0.00007	0.38357	0.04189
TST-A14	1.389	0.009	0.04590	0.00006	0.38325	0.04125
TST-A16	1.563	0.037	0.04591	0.00005	0.38348	0.04068
TST-A19	1.905	0.013	0.04588	0.00004	0.38398	0.03950
TST-A22	2.219	0.018	0.04593	0.00003	0.38352	0.03850
TST-P16	1.601	0.010	0.04589	0.00006	0.38370	0.04053
TST-P19	1.911	0.011	0.04592	0.00007	0.38387	0.03952
TST-P22	2.213	0.021	0.04592	0.00007	0.38357	0.03851

Table 1. A summary of the cable parameters and variations measured during these experiments (continued).

Cable ID	Minor Edge Packing Factor	I_c (4.22 K, 5.6T) (A)	Degrad. (%)	Modulus (MPa)
SSC-2-O-00052	0.958	9181	-0.8	-
SSC-2-O-00053	0.958	9263	-1.7	-
TST-A12	0.959	9179	-0.8	7170
TST-A14	0.973	9115	-0.1	6740
TST-A16	0.987	8970	1.49	7070
TST-A19	1.017	8819	3.15	7180
TST-A22	1.043	8545	6.16	6280
TST-P16	0.099	8953	1.68	6630
TST-P19	1.016	8846	2.86	6510
TST-P22	1.043	8665	4.84	5910

In order to verify the degree of success at modifying only the keystone angle during this experiment, both the midthickness and the width of each of the cables fabricated for this study are plotted in Figure 1. The total axis height, for both width and midthickness, is approximately the same as the range allowed by the SSC specification for these parameters. The data for the width of the cables are complicated by the fact that the CMM cannot apply a sufficient load while clamping on the edges of the cable to accurately measure the exact cable width. The measurement is a compromise between obtaining as accurate a measurement as possible and preventing buckling of the cable across the face during the measurement. As a result, the variation in the width represents a worst case situation. (Note: The present version of the CMM software performs the measurement of the cable dimensions in standard inch-pound dimensions. A new version performing SI measurements will be released prior to the start of pre-production fabrication.) The evidence indicates that this cable set does indeed represent a controlled set of samples in which the keystone angle is the only parameter that has been varied.

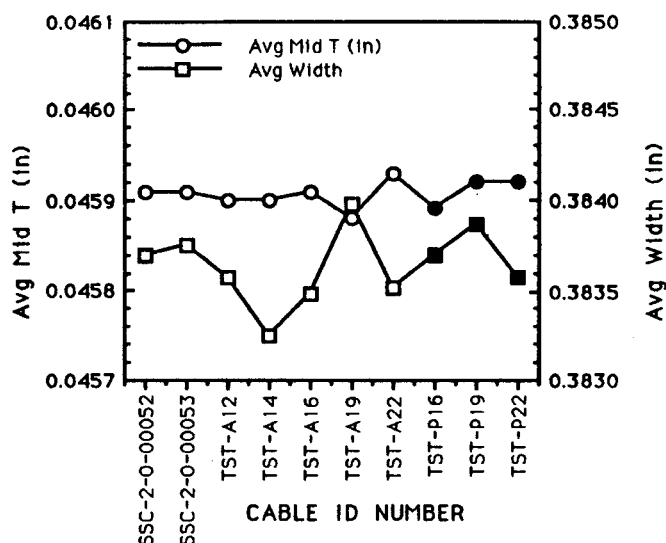


Figure 1. Average cable midthickness and average cable width plotted for each of the cables produced for this study.

METALLOGRAPHIC EXAMINATION

Representative micrographs (at a magnification of 50 \times) of the cables from these experiments are displayed in Figure 2. Figures 2a and 2b are images of the major and minor edges, respectively, of the standard 40-mm outer quadrupole cable that meets all aspects of the SSC specification. The cable has been sectioned near the location of the highest compaction of the strands on the minor edge. Features to note include the radius present at the corners of the minor edge strands, the absence of a gap between the strands near the minor edge, and the presence of deformation on the strands at the major edge. These features are all typical of standard SSC cables. Figures 2c and 2d are images of the major and minor edges, respectively, of the cables fabricated using an 81-mm pitch length and the nominal 2.2 $^{\circ}$ keystone angle. This image was selected because it represents the features that concern magnet designers. Features to note include the sharp corner apparent on one of the strands at the minor edge of this cable, the same absence of a gap between the strands at the minor edge, and the near absence of any deformation on the strands near the major edge. The region near the minor edge, in which the gap between strands is closed, extends into the cable for only a few strands in the 1.2 $^{\circ}$ keystone angle case. In the 2.2 $^{\circ}$ case, there is essentially no gap between the strands through approximately half the cable width.

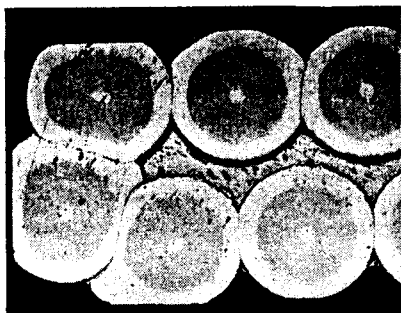


Figure 2a. Micrograph of cable major edge TST-A12 taken at a magnification of 50X.

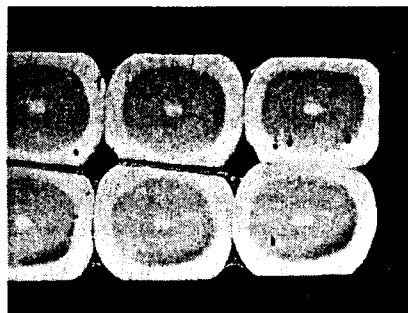


Figure 2b. Micrograph of cable minor edge TST-A12 taken at a magnification of 50X.



Figure 2c. Micrograph of cable major edge TST-P22 taken at a magnification of 50X.

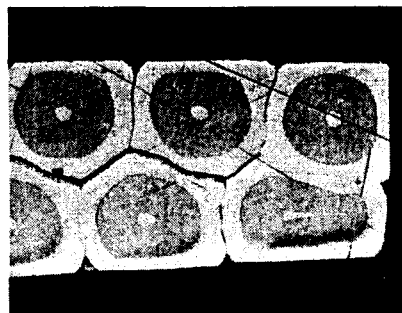


Figure 2d. Micrograph of cable minor edge TST-P22 taken at a magnification of 50X.

ELECTRICAL PROPERTIES

The critical current density of each of these cables has been measured at Brookhaven National Laboratory. Each of the cables was measured at several fields between 5 and 6 T in liquid helium. The critical current is reported at the specification field of 5.6 T, by interpolation using a linear fit, and at a temperature of 4.22 K, by correcting for measured changes in ambient pressure above the sample. The cables were mounted in the holder so that the magnetic field generated by the transport current flowing in the cable was aligned, thereby adding to the applied field at the location of the minor edge.⁶ Thus the worst-case current degradation within the cables was measured. The cable I_c has been corrected for the self-field of the cable. The cable degradation is calculated based on measurements of virgin samples of the wire used in the cable. The wire measurements have not been corrected for self-fields. Thus the total absence of degradation would manifest itself as a reported degradation of approximately -4.0%.⁶

The electrical behavior of the cables as a function of increasing keystone angle is shown in Figure 3a, and the resulting I_c degradation as a function of increasing keystone angle is shown in Figure 3b. Cables with the standard pitch length of 73 mm are displayed as open circles; cables with the lengthened pitch of 81 mm are displayed as closed circles. Of note are the extremely low values of degradation achieved for the three cable samples fabricated to the latest SSC specifications.

A comparison of these data with the 36-strand cables produced using the same batch of wire on the same cabling machine² reveals that equivalent values of degradation have been achieved in the 30-strand cables and in the 36-strand cables. This somewhat surprising result, it is believed, is primarily due to the optimization of the rollers dimensions prior to the start of these runs. In

addition, it demonstrates that once sufficient experience is obtained with a particular cable type, manufactured on a particular machine, it is possible to reduce degradation to similar levels, independent of the aspect ratio of the cables. This result reinforces the validity of the cable scaling guidelines described in Ref. 3, and the learning curve effects demonstrated in Ref. 4.

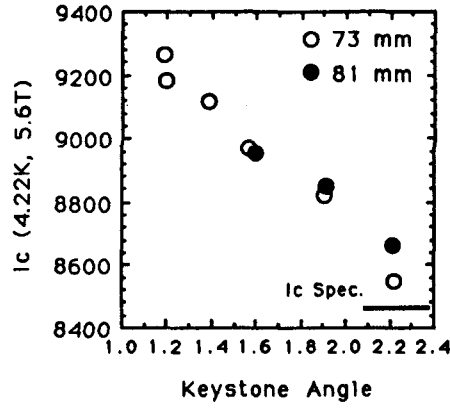


Figure 3a. Critical current measured at 5.6 T and 4.22 K plotted against cable keystone angle for both the 73-mm and 81-mm pitch lengths.

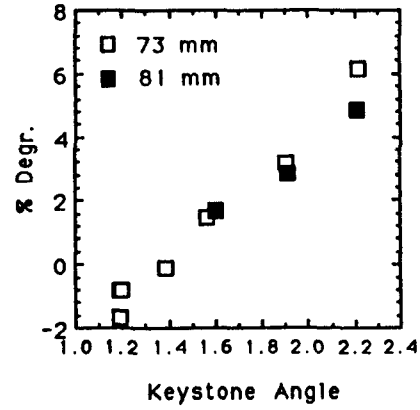


Figure 3b. Degradation plotted against cable keystone angle for both the 73-mm and 81-mm pitch lengths.

Cable degradation has often been discussed in terms of the minor edge packing factor (PF_t), which relates the compaction of the strands along the minor edge to the area of the virgin strand. The expression for the packing factor is given by the formula:

$$PF_t = 2\pi D/t, \text{ where } D \text{ is the wire diameter and } t \text{ is the minor edge thickness of the cable.}$$

The degradation data plotted against the minor edge packing factor is shown in Figure 4. Of interest are the significantly smaller values of degradation achieved in this case compared with the data obtained on similar 30-strand cables.²

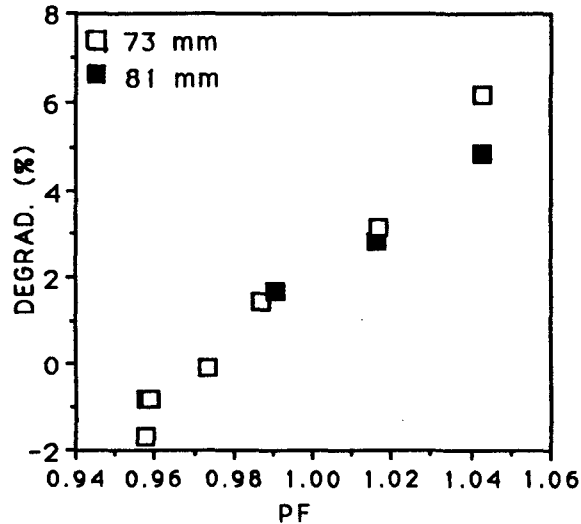


Figure 4. The degradation data plotted against the minor edge packing factor.

Upon analysis of the cable data for the cables used for the ASST, it is obvious that a parameter besides the minor edge packing factor controls the degradation. The complete set of data is presented elsewhere in this conference proceedings.² As shown in that publication, the level of degradation achieved for a given manufacturer's wire is directly related to the design of the strand cross section.

Of particular importance to the degradation is the distance the outermost filaments are from the outer surface of the strand. The closer to the outside of the strand the filaments are, the less copper is available to absorb the deformation of the strand resulting from the cabling operation. In addition, the filaments near the outside of the wire are subjected to higher bending and twisting stresses as they get closer to the outside surface in the strand design. We have parameterized this effect by using the ratio of the minimum distance the outermost filaments are from the outside surface of the strand, r , and the diameter of the strand itself, D .

The data presented in this paper and the data of Ref. 2 lead to the deduction that the degradation vs. PF_t is, in reality, a family of curves each having the same general shape. However, the design of the strand, described through the parameter r/D , serves to shift values of degradation to either higher or lower values of PF_t , depending on whether r/D is smaller or larger, respectively.

MECHANICAL PROPERTIES

A 10-stack of the test fixture was used to measure the modulus of 10-stack specimens of the (uninsulated) cables produced in this program. In this fixture, 10 short samples of cables were loaded in such a way as to alternate the major and minor edges of the cable. This geometry allows the total sample to remain approximately rectangular in shape. The geometry also simplifies the tooling required compared to that necessary for the curved geometry that would result in aligning the narrow edges within the fixture.

All tests reported here were performed on uninsulated cable, with no heat treatments to simulate any type of coil curing cycle. All of the modulus measurements were performed at room temperature. All of the reported data were obtained under condition of increasing compressive load.

The following test procedure was utilized in the determination of the modulus of the cable 10-stacks: 1) The gage bar was inserted into the fixture, and a load was applied equivalent to a pressure of 6.34 MPa at the load surface. The gage bar was verified to be at approximately the height of a lightly compressed 10-stack (12.7 mm in this case). 2) The deflection gages were zeroed at this point, the machine was unloaded, and the gage bar was removed. 3) The 10-stack cable sample was loaded into the fixture. 4) A stable load, equivalent to 6.34 MPa of pressure, was applied while recording the deflection gage readout (used later to determine the initial stack height). 5) The applied load was increased at a rate of 4.448 kN/s to a maximum load equivalent to 102 MPa. The stress data were collected during the ramp at a rate of 1 data point/s. 6) The machine was unloaded, and the sample removed and archived for later examination. 7) Finally, the gage block was reinserted, the applied load was increased to 6.34 MPa pressure equivalent, and the deflection gage zero was checked for comparison to the initial value. This procedure was repeated for each of the measured samples.

The behavior of the 10-stack moduli as a function of increasing keystone angle is shown in Figure 5. Several trends can be deduced from the data: First, there is a noticeable decrease in the 10-stack modulus for keystone angles beyond 1.9° for both pitch lengths examined. Second, the 10-stack modulus is lower for the cables produced with the longer pitch length for the range of keystone angles examined. Finally, for both pitch lengths, one can infer from the data that, in general, the 10-stack modulus is approximately constant up through keystone angles near 1.9° for both pitch lengths.

Work is continuing in the area of understanding the mechanical properties of the cables as a function of keystone angle. Particular attention will be focussed on the effects of thermal treatments that simulate the coil curing process. These results will be published in future work.

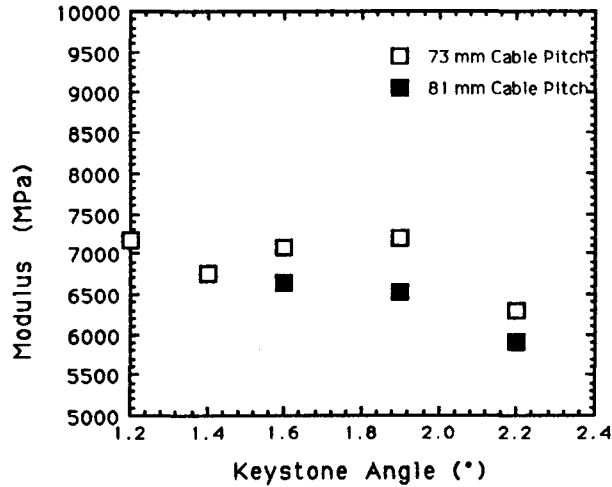


Figure 5. Cable 10-stack modulus plotted against keystone angle for both the 73-mm and 81-mm pitch lengths.

SUMMARY

This paper demonstrates the capability of expanding the design window available to magnet designers. Under controlled conditions, a series of cables were successfully produced that provide the ability to form wedgeless coil cross sections. Through the entire range of keystone angles examined, electrical and mechanical properties within acceptable limits were achieved. Several issues of concern when moving into the range of large keystone angles have been identified. However, based on these results, acceptable quad cables can be produced with angles near 1.9°, and perhaps beyond.

In determining the properties of these cables we have demonstrated that strand design, in addition to the minor edge packing factor, plays a major role in determining the level of degradation achieved in SSC-type cables. The mechanical properties of these cables have been found, thus far, to vary in a systematic and gradual manner, so that only moderate changes in coil properties are expected as a result of the changes.

Work is now underway to develop alternate 2D cross sections for the SSC quadrupole magnet that take advantage of the increased design flexibility available. Cables will be produced during the coming months for the fabrication of several model magnets using cables with increased keystone angles. Results of this work will be published.

ACKNOWLEDGMENTS

The authors gratefully acknowledge discussions with J. Waynert and W. Nick from the B&W/S team, along with the support of the SSC quadrupole product manager, S. Shapiro. The authors are also grateful for the tremendous effort made by M. Garber of Brookhaven National Laboratory in providing the cable I_c test results in such a short amount of time.

REFERENCES

1. SSC Cable Specification M30-000287, Superconducting Cable for SSC Quadrupole Magnets.
2. D. Christopherson, D.W. Capone II, C.R. Hannaford, S. Graham, and D. Pollock, "Summary of the Superconducting Cable Produced for the Accelerator System String Test Program."
3. J. Royet and R. M. Scanlan, "Manufacture of Keystoned Flat Superconducting Cables for Use in SSC Dipoles," *IEEE Trans. on Magnetics*, **MAG-23**, 480 (1987).
4. R.M. Scanlan and J. Royet, "Recent Improvements in Superconducting Cable for Accelerator Dipole Magnets," Preprint.
5. S.A. Gourlay, M. Garber, J. Royet, and R.M. Scanlan, "Degradation Studies of Fermilab Low Beta Quadrupole Cable," *IEEE Trans. on Magnetics*, **MAG-27**, 1815 (1991).
6. M. Garber, A.K. Ghosh, and W. B. Sampson, "The Effect of Self Field on the Critical Current Determination of Multifilamentary Superconductors," *IEEE Trans. on Magnetics*, **MAG-25**, 1940 (1989).